ACS APPLIED MATERIALS & INTERFACES

Research Article

www.acsami.org

Cold Crystallization of Glassy Polylactide during Solvent Crazing

Elena S. Trofimchuk,*[,†] Alexander V. Efimov,[†] Tatiana E. Grokhovskaya,[†] Nina I. Nikonorova,[†] Marina A. Moskvina,[†] Nikita G. Sedush,[‡,§] Pavel V. Dorovatovskii,[‡] Olga A. Ivanova,[†] Ekaterina G. Rukhlya,[†] Aleksandr L. Volynskii,[†] and Sergey N. Chvalun*[,‡]

[†]Department of Chemistry, Moscow State University, 1/3, Lenin Hills, Moscow 119991, Russia

[‡]National Research Centre "Kurchatov Institute", 1, Akademika Kurchatova pl., Moscow 123182, Russia

[§]Moscow Technological University, Institute of Fine Chemical Technology, 86, pr. Vernadskogo, Moscow 119571, Russia

Supporting Information

ABSTRACT: Uniaxial tension accompanied by the orientation and crystallization of polymer chains is one of the powerful methods for the improvement of mechanical properties. Crystallization of amorphous isotropic polylactide (PLA) at room temperature is studied for the first time during the drawing of films in the presence of liquid adsorption-active media (ethanol, water−ethanol mixtures, and *n*-heptane) by the solvent crazing mechanism. The crystalline structure arises only under simultaneous actions of a liquid medium and a tensile stress and does not depend on the nature of the environment. The degree of polymer crystallinity increases nearly linearly with the growth in the fraction of the fibrillar material and reaches a maximum value of 42−45%. It has been stated that polymer crystallization happens in crazes involving nanofibrils with a diameter of about 10−20 nm without affecting the bulk polymer parts. Wide-angle X-ray scattering has been used to confirm that the crazing-induced crystallization is accompanied by the formation of the α'-crystalline phase with crystallite sizes (X-ray coherent scattering region) of 3−5 nm, depending on the nature of the liquid medium. After stretching in liquid media to a high tensile strain, the strength of a PLA film has increased to 200 MPa.

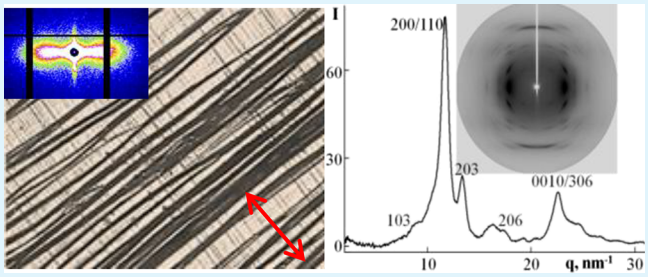

KEYWORDS: *polylactide, solvent-crazing, crystallization, liquid environment, drawing, uniaxial stretching*

1. INTRODUCTION

Biopolymer polylactide or poly-lactic acid (PLA) is a commercially attractive aliphatic polyester, as lactide is available from the renewable plant sources.[1,2] It is an environmentally safe and nontoxic material, unlike most commercial-grade plastics. PLA can degrade upon exposure to a wide variety of microorganisms and is able to bioresorbate in vivo until complete dissimilation. Thus, PLA is a promising material to be used as composite matrices applied in biomedicine and as an alternative to traditional slowly degradable package materials and so forth.[3,4]

Frequently, the main drawback of PLA (especially for pure poly-L-lactic acid and PLA containing several percent of D-lactic acid units) is its brittle fracture behavior under room conditions, while the maximal degree upon stretching usually does not exceed 10−15%,[5,6] which restricts its application. Main causes of PLA embrittlement include fast physical aging[7,8] together with structuration and formation of nucleation centers in the brittle cracks. Thus, solving this problem is an important and demanded task. Lately, a large number of research studies dealing with different methods for reducing the brittleness and increasing the strength of polylactide appeared. The common approaches were the addition of softeners,[9−11] the short-term thermal treatment at the glass-transition temperature,[12,13] and the orientation at high temperatures.[14] Orientation drawing at an elevated temperature (commonly, near or slightly higher than the glass-transition temperature (T_g)) is one of the powerful methods usually accompanied by orientation and crystallization of the polymer chains. The high strength (up to 1 GPa), elasticity, and thermal stability of oriented crystalline fibers and films are the reasons for increased interest in the study of orientation and crystallization of PLAs.[15,16]

Isotropic PLA has a rather low crystallization rate, even at temperatures above its glass transition. Crystallization of PLA depending on its molecular structure, content of nucleating agents and plasticizers, and processing conditions has been studied in a number of works.[14,17−21] Tensile-stress-induced orientation of PLA above its glass-transition temperature substantially increases its ability to crystallize. For example, the crystallization rate and the degree of crystallinity of the polymer increase compared to those of unoriented PLA. At elevated temperatures, PLA may crystallize into different crystalline forms. The α (or α') crystalline form is the most thermodynamically stable one. It was for the first time

Received: July 4, 2017
Accepted: September 12, 2017
Published: September 12, 2017

DOI: 10.1021/acsami.7b09666
ACS Appl. Mater. Interfaces 2017, 9, 34325−34336

described in refs 17 and 22 and is characterized by an orthorhombic cell and a chain conformation having the shape of a 10/3 helix. This crystalline form can be obtained by stretching PLA at relatively low strain rates and temperatures of 70−90 °C. The same crystalline modification results from the thermal crystallization of isotropic samples at temperatures higher than 120 °C. Direct investigations performed by small- and wide-angle X-ray scattering (SAXS and WAXS, respectively) measurements have shown that the uniaxial deformation of amorphous PLA films at 80 °C yields a more disordered α'-crystalline phase with the "shish-kebab" morphology.[23] Polymer stretching at high strain rates and a temperature close to the melting point (170 °C) up to very high tensile strains (by 10−20 times) gives rise to the formation of the β-crystalline form with orthorhombic cells and the conformation of a 3/1 helix.[24,25]

The uniaxial PLA deformation near to the glass-transition temperature (65 °C) is accompanied by the gradual enhancement of molecular orientation in an amorphous polymer and, starting from a tensile strain of approximately 100%, the formation of a mesophase with a content around 10−15% prior to the rupture of a sample.[26] The authors[27] have reported that mesocrystals begin to arise with the critical degree of amorphous phase orientation equal to approximately 0.45, and the strain necessary for the appearance of the mesocrystals increases with the stretching temperature. The formation of the PLA mesophase is often observed upon crystallization of PLA bulk copolymers from melts. The heating of the mesophase leads to the improvement of its crystalline structure and the formation of the α-crystalline phase.[28]

Structural rearrangements in PLA during its uniaxial deformation in air below T_g (at 35 and 45 °C) have been studied.[29] Polymer deformation under these conditions occurs together with necking, while a high molecular orientation of PLA chains was found in the neck according to the WAXS data. Differential scanning calorimetry (DSC) was employed to study the thermal behavior of samples stretched with the formation of necks at 45 °C (15 °C lower than T_g) by 160 and 200%. The preliminary orientation of macromolecular chains substantially increases the rate of polymer crystallization. For example, a wide exothermic peak appeared in a temperature range of 75−140 °C[29] because of the cold crystallization of PLA that stretched into a neck.

In this work, we propose to use the solvent-crazing process[30−32] to reduce the PLA fragility and to increase its strength characteristics. Crazing of polymers is a fundamental mechanism of plastic deformation of solid amorphous and semicrystalline polymers, and it is accompanied by the formation of an oriented highly dispersed fibrillar−porous structure in local deformation zones, which are referred to as crazes.[33,34] Moreover, it is known[35−38] that crazing is considered as a method for loading polymer matrices with different thermodynamically incompatible low- and high-molecular additives, such as dyes, fire-retardant agents, odorants, bactericides, and so forth, with a simultaneous dispersion of fillers up to the nanometric level.

Previously,[39] we studied the mechanical behavior of a commercial film of glassy poly-L-lactic acid during its drawing under room conditions in the presence of various liquid media (aliphatic hydrocarbons and alcohols). The stress−strain test and optical microscopy justified that PLA is deformed via the crazing mechanism with the formation of a highly dispersed fibrillary−porous structure with fibrils of about 20 nm diameter, according to the SAXS data. Moreover, an increase in the elongation at the break of PLA to 500% occurred upon stretching in the presence of ethanol. Furthermore, at high tensile strains (higher than 300%), the DSC thermogram showed the formation of a crystalline structure of PLA with a degree of crystallinity of about 35%. It is worth noting that the orientation drawing of polyethylene terephthalate (PET, which has properties similar to PLA) to high tensile strains (300−400%) under same conditions also results in the development of the crystalline structure.[40−42]

Earlier, solvent crazing was also used to introduce starch and calcium phosphates into the PLA matrix.[43] As a result, nanocomposite materials with bioactive properties, in particular, with osteoconductive properties toward pre-osteoblastic MC3T3E1 cells were obtained.

The obtained data[39,43] initiated systematic research studies of PLA crystallization features during solvent crazing. The aim of this work is to study the peculiarities of the crystallization process of glassy PLA during uniaxial stretching of its isotropic film in different liquid environments at room temperature (35−40 °C lower than the glass-transition temperature). Determining the conditions of crystallization and the type of a PLA crystalline structure formed under these conditions and its influence on the development and stabilization of the fibrillar−porous structure are the desired main objectives.

2. EXPERIMENTAL SECTION

Initially, a PLA film with 110−140 μm thickness was obtained by the hot-pressing procedure from pellets of the grade 4032D (NatureWorks LLC, United States). The polylactide has the following characteristics: molecular mass M_w of 200 kDa, polydispersity index of 1.6, the content of D-isomer units equals to 2%, glass-transition temperature of 63−65 °C, and melting temperature of 168 °C. After the PLA pellets were melted and pressed in a mold, the sample was rapidly quenched with water at 15 °C. During quenching, the polymer film surface had no direct contact with water. This approach yielded amorphous isotropic samples. Before the experiments, the obtained PLA films were exposed under room conditions for at least 2 weeks. Some polymer samples were annealed at 80 °C followed by quenching and were used immediately after cooling.

The as-prepared PLA films were uniaxially stretched in air and different liquid media. The media were selected from organic liquids, namely, from hydrocarbons and aliphatic alcohols, which are most frequently used as adsorption-active media (AAMs) to realize solvent crazing in polymers. By definition, AAMs are media that cause none or insignificant swelling of polymers (commonly the degree of swelling in them is no higher than 10 wt %) but efficiently reduce their surface energy. Therefore, PLA swelling was studied in different AAMs. An initial polymer film was placed into selected liquids at room temperature or at 50 °C and exposed until the maximum constant mass of the sample was reached. Initial and swollen samples were weighed using an AND ER182A electronic balance with an accuracy of ±0.0001 g. The equilibrium degree of swelling (dm/m_o, %) was calculated as follows

$$\frac{dm}{m_0} = \frac{m - m_0}{m_0} \times 100 \quad (1)$$

where m_o is the initial mass of the film and m is the mass of the swollen film. We have chosen n-heptane (analytical grade) and 96% ethanol from hydrocarbons and aliphatic alcohols, respectively. In addition, water−ethanol mixtures with ethanol contents ranging from 20 to 50 vol % were used.

For mechanical tests, standard dumbbell shaped samples with the working part sizes of 6 × 20 mm were cut of the initial films. The orientation stretching was performed at room temperature at a rate of 5 mm/min (25%/min) with an Instron 4301 tensile machine. To carry

DOI: 10.1021/acsami.7b09666
ACS Appl. Mater. Interfaces 2017, 9, 34325−34336

out the mechanical test in the presence of AAM, samples from the initial PLA film were clamped into a special device of the tensile machine, immersed in a liquid medium, and immediately deformed.

The appearance of the deformed samples was recorded with a Sony digital camera. The surface morphology was studied with a Carl Zeiss Jena optical polarizing microscope, whereas the volume morphology was examined using an EVO 40 XPV scanning electron microscope (SEM; Zeiss) equipped with an XFlash 6130 attachment for X-ray spectroscopic microanalysis (Bruker). For this purpose, cleavages were prepared from deformed samples by brittle fracture along the direction of stretching in liquid nitrogen. The cleavages were attached to the surface of a special microscope table with conducting carbon double-sided sticky tape, and a gold layer 50−70 nm thick was sprayed onto them with a Giko IB-3 setup.

Calorimetric measurements were performed on a Mettler DSC-20 differential scanning calorimeter in a range of 25−200 °C at a heating rate of 10 °C/min in a nitrogen atmosphere. Before the calorimetric test, the samples were dried immediately after drawing as rapidly as possible to constant weight under vacuum. This procedure allowed us to minimize changes in the degree of crystallinity and the influence of the evaporation of solvents on the thermal properties of PLA. The degree of crystallinity of the PLA samples was derived from the DSC data by calculating the heat effects of polymer melting and crystallization using the software of the processor supplied with a Mettler-TC11 instrument. The degree of crystallinity (α, %) was calculated by the following formula 2

$$\alpha = \frac{\Delta H_{m} - \Delta H_{cr}}{\Delta H_{100\%}} \times 100 \quad (2)$$

where ΔH_{m} and ΔH_{cr} are specific heat effects of sample melting and crystallization, respectively, and $\Delta H_{100\%}$ is a specific theoretical melting enthalpy of 100% crystalline polymer (for PLA, 93 J/g[44]).

The structures of initial and stretched PLA films were investigated by the WAXS technique. X-ray scattering patterns were obtained using the Station "Belok" at Kurchatov Centre of Synchrotron Radiation, Moscow, Russia (beamline 4.4e of Kurchatov Synchrotron radiation source) equipped with a Rayonix SX165 detector operating at a resolution of 2048 × 2048 pixel (pixel size was 80 μm). The sample−detector distance was 150 mm. The synchrotron radiation wavelength was 0.0987 nm. Radial intensity profiles, $I(2\theta)$, were obtained by 180°-azimuth integrations of the 2D-patterns over 180° by means of the Fit2D software. The obtained X-ray scattering curves were plotted in the intensity−scattering vector units, with the vector being calculated as follows

$$q = \frac{4\pi \cdot \sin(\theta)}{\lambda} \quad (3)$$

where θ is the Bragg angle and λ is the radiation wavelength. Figure 1 shows fitting azimuth-integrated WAXS profiles of a sample stretched to 230% in *n*-heptane. The weight fractions of the amorphous and crystalline phases were quantitatively assessed with the help of a previously described method[26] using the PeakFit software assuming Gaussian profiles for all scattering peaks and amorphous halo. An example of fitting azimuth-integrated WAXS profile of an experimental scattering curve in terms of Gaussians is presented in Figure 1.

The degrees of crystallinity of the deformed PLA films were computed from the ratio of the Bragg scattering contribution of the crystalline phase to the total scattering intensity by the following equation

$$\alpha = \left(1 - \sum \frac{S_{am}}{S_{total}}\right) \cdot 100 \quad (4)$$

where S_{am} refers to the areas of the Gaussian peaks attributed to the amorphous halo (their positions are determined from the integral scattering curve plotted for an initial amorphous film) and S_{total} is the total area under the integral scattering curve.

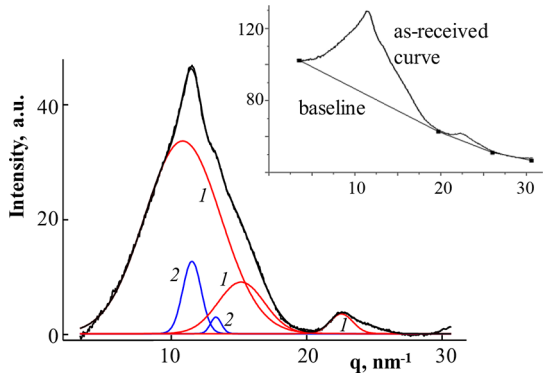

Figure 1. Example of PeakFit treatment of the azimuth-integrated WAXS profile of PLA sample stretched in the presence of *n*-heptane by ε = 230%. Curves 1 (red lines) are related to the amorphous phase and curves 2 (blue lines) are related to the crystalline phase.

The crystal size (coherent-scattering region) was calculated from the full widths at half-maximum (fwhm) of the fitted crystalline peaks using the Debye−Scherrer equation expressed as follows[45]

$$D_{hkl} = \frac{K\lambda}{\beta_{1/2} \cos\theta} \quad (5)$$

where D_{hkl} represents the average crystallite size in the normal direction of the (200/110) reflection plane and $\beta_{1/2}$ is the fwhm of the diffraction peak (200/110) in radians. Shape factor K was preset to be 0.9 for polymer systems, whereas the instrumental resolution was neglected.

The disorientation angle of PLA crystallites with respect to the drawing direction of the polymer was defined as the integral azimuthal half-width of the (200/110) reflection.

The SAXS was measured at DIKSI beamline[46] for the Kurchatov Centre of Synchrotron Radiation (Moscow, Russia). The beamline utilizes an X-ray wavelength of 0.16 nm and a vacuum chamber length of 2.4 m, which allows measuring SAXS in the q range of 0.07−1.1 nm^{-1}. For calibration of the scattering vector interval, the silver behenate standard was used.[47] To obtain the scattering pattern, the wet polymer samples were clipped in special clamps at fixed tensile strain. The scattering was measured by using a Dectris PILATUS3R 1 M detector with 300 s exposition and then treated by FIT2D software to obtain 1D scattering intensity versus scattering vector module, $I(q)$, curve. The pixel size on the scattering pattern is 172 μm. Using the obtained equatorial scattering curve $I(q)$, the average diameter of fibrils spanning walls of the craze was determined. The details of the calculation method are described in the Supporting Information (section S2, pages S-3−S-5).

3. RESULTS AND DISCUSSION

3.1. Mechanical Behavior of PLA Films in Liquid Environments. The mechanical behavior under standard conditions of the original PLA film obtained in this work was similar to that previously observed.[12,48] Figure 2 shows a typical engineering stress−strain curve (1) for an amorphous PLA film that has a plastic yielding value of about 60 MPa and a breaking strain of no higher than a few tens of percent (in this case, 30%). The image of this sample is depicted at the curve. The entire working part of the sample is covered with craze-type cracks, the formation of which occurs at the surface microdefects near the plastic yielding ε = 2−3% and proceeds to the development of a true rupture-related crack. This rupture mechanism is typical for glassy amorphous polymers and has been previously described in a number of works.[49,50]

The deformability of a PLA film can be increased by heating at a temperature in the vicinity or slightly higher than the glass-

DOI: 10.1021/acsami.7b09666
ACS Appl. Mater. Interfaces 2017, 9, 34325−34336

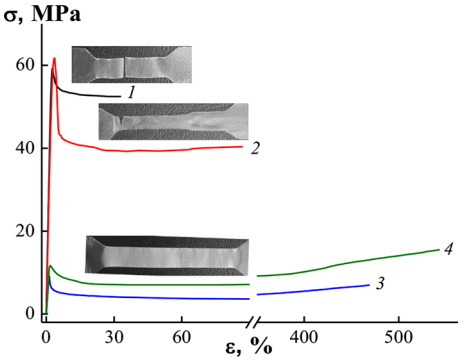

Figure 2. Stress–strain curves for the original (1, 3, 4) and annealed at 80 °C during 0.5 h (2) PLA films recorded in the presence of air (1, 2), *n*-heptane (3), and 50% water–ethanol mixture (4). Over stress–strain curves, the photographs of the post-mortem tensile test samples are presented for (1) and (2) at breaking and for (3) after stretching to 50%.

transition temperature (70–80 °C) for a rather short time period (0.5–1 h).[12,51] The annealing under these conditions does not lead to a noticeable increase in the degree of polymer crystallinity, but it causes the healing of defects that are transformed into the sites of craze nucleation under load. Figure 2 illustrates the stress–strain curve (2) and the appearance of a PLA film deformed after annealing. The breaking strain is much higher (up to 120%), and the deformation mechanism is different. The stretching of the annealed PLA film is accompanied by the formation of a transparent neck with a characteristic abrupt narrowing of the working part of the dumbbell samples. The neck tensile strain determined from a change in the sample sizes is nearly 250%. The repeated mechanical test of an annealed PLA sample after several days shows a substantial decrease of the breaking strain value. This behavior is typical for some amorphous glassy polymers such as PET or polycarbonates because of the processes of physical (structural) aging.[52,53]

The drawing of the original unannealed aged PLA films at room temperature in the presence of liquid media is also accompanied by a substantial increase in the breaking strains (up to 500%), which was recently reported.[39] As it can be clearly seen from Figure 2 (curves 3, 4), a PLA film is indeed stretched in both *n*-heptane and a 50% water–ethanol mixture at approximately fourfold lower stresses than it is in air and is characterized by a substantial increase in the deformability. Under these conditions, the crazing mechanism of deformation dominates. Commonly, the presence of liquid media[30−32] substantially facilitates the crazing process and decreases the mechanical strength of solid polymer materials during their utilization. The problems relevant to the determination of the mechanism for the effect of a liquid environment on the processes of craze formation were discussed in detail earlier.[30,54] The main role of an AAM is to reduce the surface energy at the polymer–liquid interface because of the adsorption of liquid molecules on the surface of a polymer material and to stabilize the newly formed thin fibrils. Thus, the surface tension of polyesters such as PET or PLA may be decreased in liquid environments by almost ten times.[55]

Optical micrographs of the surface (Figure 3), at the initial stages of deformation in the region of plastic yielding, show that the working part of the PLA film is covered by numerous cracks (crazes) oriented normally to the stretching direction and separated by regions of the bulk unoriented polymer. After the removal of the AAM by evaporation under isometric conditions from the as-formed crazes of PLA, the samples become white. The crazes gradually widen because of the involvement of the bulk polymer parts during the deformation process (Figure 3b). At large tensile strains (200–400%), after almost all bulk regions have passed to the crazes, the crazed porous structure collapses (Figure 3c) and the samples become transparent.

Similar to other amorphous glassy polymers (e.g., PET stretched in alcohols[30,56]), the formation of an oriented and highly dispersed fibrillary–porous structure in PLA by the crazing mechanism and the evolution of this structure with increase in the tensile strain fits all observed phenomena. SEM images (Figure 4) have confirmed the assumption that the

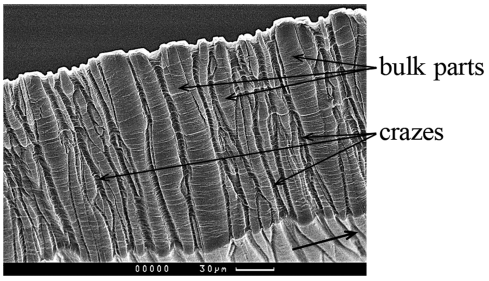

Figure 4. SEM micrograph of the fragile cleavage of the PLA film stretched by 100% in 50% water–ethanol mixture.

stretching of a PLA film in different liquid media leads to the formation of crazes, which grow through the entire cross section of a sample. The micrograph clearly shows the pronounced alternating regions of the bulk polymer and the porous material (crazes), which is similar to those previously obtained for other amorphous glassy polymers (PET, poly(vinyl chloride), etc.) stretched via the crazing mechanism.[30,57]

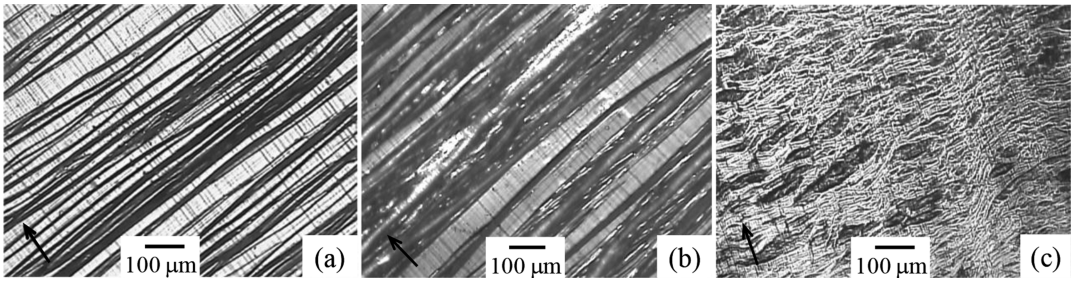

Figure 3. Optical micrographs of the surface (magnification 50 times) PLA films deformed in the presence of *n*-heptane by 50 (a), 150 (b), and 230% (c). The stretching direction of the film is indicated by the arrow.

DOI: 10.1021/acsami.7b09666
ACS Appl. Mater. Interfaces 2017, 9, 34325–34336

The effective volume porosity of such films depends on the tensile strain and may be as large as 60 vol %.

The SAXS study of the deformed PLA samples has also confirmed the formation of the crazed fibrillary–porous structure. Figure 5 shows the 2D SAXS pattern of the PLA

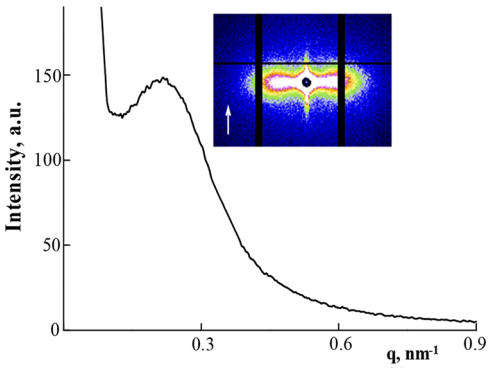

Figure 5. Equatorial distributions of the SAXS intensity for PLA deformed by 100% in 50% water–ethanol mixture. In the inset, the 2D SAXS pattern is presented. X-ray-shooting was carried out in liquid. The arrow shows the direction of the PLA tension.

film stretched in 50% water–ethanol mixture and its corresponding curve of equatorial distributions of intensity. For comparison, the 2D SAXS pattern of the initial PLA film (presented in the Supporting Information, Figure S1) exhibits a slight diffuse scattering near the center with almost uniform intensity distribution over the circle, which indicates the absence of an ordered structure and confirms that the film obtained by the hot-pressing method is isotropic. The deformation of PLA in the liquid environment changes the scattering pattern strongly. Such a scattering pattern is typical of craze-containing glassy polymer systems[58,59] and consists of two reflections (Figure 5, inset). The meridional component of the scattering arises because of the X-ray reflection from craze walls oriented perpendicular to the stretching direction. The anisotropic reflection on the equator is due to the X-ray diffraction on the system of fibrils spanning the craze walls. The fibrils are oriented in the stretching direction and separated in space.

The equatorial component of SAXS of the deformed PLA (Figure 5) contains the interference peak. The angular position of the maximum is 0.22–0.24 nm^{-1}, which corresponds to the value of the long period of 26.0–28.5 nm. Here, the value of the long period characterizes the distance between the centers of fibrils, namely, the sum of diameters of pores and fibrils. The presence of the maximum on the scattering curve indicates a highly regular arrangement of the separated fibrils in crazes. The Porod method modified for oriented systems[60] allows determining the diameter of PLA fibrils spanning walls of crazes. A thorough description of such a mathematical method of calculation is presented in the Supporting Information (section S2). In this calculation, we assumed that the concentration of fibrils in craze (c) is the inverse of the extension ratio of fibrils (λ), that is, $c = 1/\lambda$. Usually, λ corresponds with a good accuracy to the natural draw ratio in the neck.[40,54] The obtained values show that the natural draw ratio in the neck of PLA is about 3.5, and the concentration of fibrils is 0.29. The calculated diameter of PLA fibrils in crazes appeared to be nearly 12 nm, and the diameter of pores is about 15 nm.

It can be stressed that after stretching in liquid media to a high tensile strain and drying under vacuum to the constant weight, the strength of a PLA film (the stress–strain curve is presented in Figure 6) has increased to 200 MPa versus about

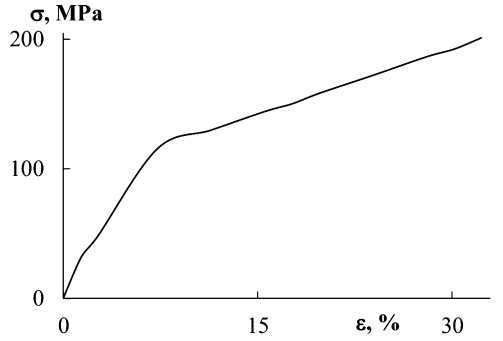

Figure 6. The stress–strain curve of the PLA film after drawing by 400% in ethanol and removal of the solvent.

60 MPa for the initial PLA film. It was previously reported[5] that the tensile strength for films and fibers of PLA could be increased using orientational stretching to 400–600% at temperatures of 70–90 °C in air. The improvement in mechanical properties was associated with the formation of a highly oriented crystalline structure in the polymer.

Thus, the uniaxial stretching of an amorphous isotropic PLA film in different liquid media (saturated hydrocarbons, aliphatic alcohols, and alcohol–water mixtures) proceeds via the crazing mechanism and is accompanied by the formation of the high-dispersed fibrillar–porous structure, typical of solid amorphous polymers. However, the reason for the dramatic increase in the deformability of PLA (sometimes, up to 550%) remains to be clarified. Undoubtedly, one of the causes may be the drastic (four or five times) decrease of the mechanical stress of deformation in the presence of liquid media. Crystallization while crazing is another possible reason for the high stability of the formed PLA fibrils (similar to PET). To verify this assumption about the crystallization of PLA fibrils below T_g during the uniaxial stretching in liquid media, the thermal properties of the deformed samples were studied by DSC.

3.2. Study of Thermal Properties of the Deformed PLA Films. DSC is an informative technique that allows not only to determine the characteristic thermal transitions in a polymer material (glass transition, crystallization, or melting) but also to evaluate the degree of polymer crystallinity. Figure 7a,b presents the DSC curves for an original PLA film and the film after its stretching to different tensile strains in ethanol or *n*-heptane followed by drying at room temperature under isometric conditions. The initial undeformed PLA film (tensile strain of 0%) is characterized by the following thermal transitions: glass transition at T_g = 62–64 °C; cold crystallization, which begins at a temperature higher than 80–85 °C (the crystallization peak is observed at 115 °C, and the crystallization heat effect is 18–20 J/g); and the melting of the crystalline phase at 170 °C (the enthalpy is 19–21 J/g). The starting degree of crystallinity calculated for the original film from the DSC data indicates an insignificant amount of a crystalline phase (about 1–2%). It is worth noting that the crystallization rate for PLA of this type seems to be low indeed. For example, it has been found that, at the heating rate elevated to 100 °C/min, the peaks of crystallization and melting disappear in the DSC curve, whereas the heat effect of these

DOI: 10.1021/acsami.7b09666
ACS Appl. Mater. Interfaces 2017, 9, 34325–34336

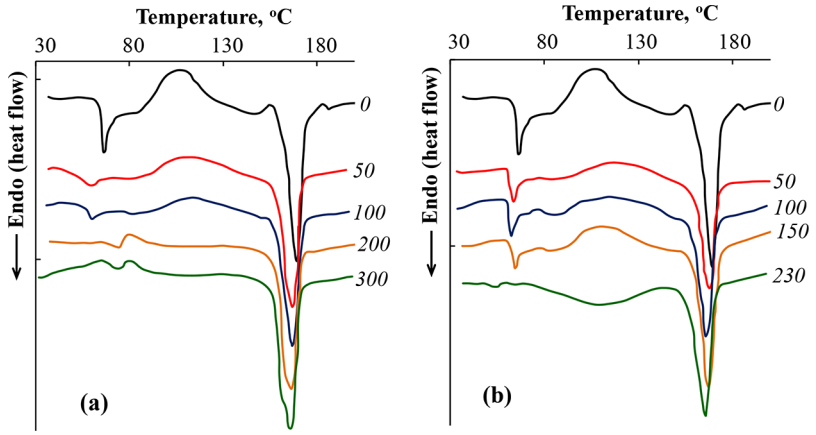

Figure 7. DSC curves of the original film and uniaxially stretched PLA to 50−300% in the presence of ethanol (a) and *n*-heptane (b). The tensile strain of samples is shown near the corresponding curve.

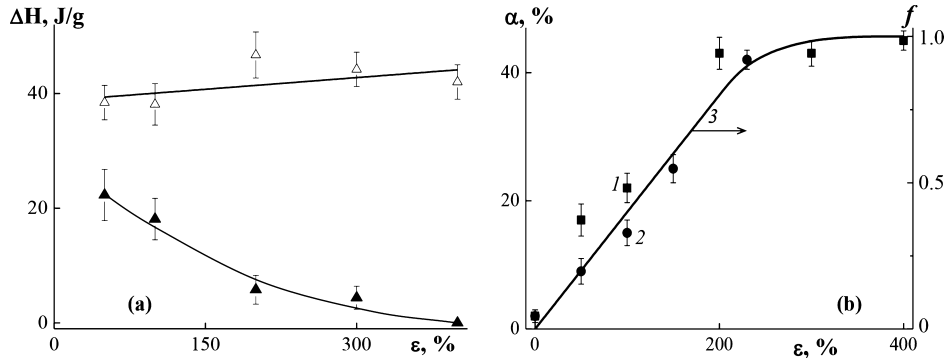

Figure 8. (a) Heats of crystallization (1) and melting (2) of PLA film vs the tensile strain of a polymer during stretching in the presence of ethanol. (b) Degree of crystallinity of PLA vs the tensile strain upon its deformation in ethanol (1, square point) and *n*-heptane (2, round point) and the fraction of the polymer material that has passed into the crazes (3, solid line) vs the tensile strain.

processes is as low as 1 J/g. Another peculiarity of the initial film is the existence of an intense asymmetric endothermic peak in the region of the glass-transition temperature. This peak can be attributed to the high rate of the physical aging of PLA.[7,8] In this case, the endothermic peak results from the decreased enthalpy of the polymer because of the improvement of its molecular packing or an increase in the concentration of low-energy conformations during storage even at temperatures lower than T_g.

Increasing the tensile strain of PLA films that uniaxially deformed in liquid media shows a gradual decrease in the enthalpy of their crystallization upon heating in the DSC cell. The dependences of the heat effects of crystallization and melting on the tensile strain upon polymer deformation in ethanol are presented in Figure 8a. Indeed, the ΔH_{cryst} value decreases from approximately 22 J/g for the sample with a tensile strain of 50%, which corresponds to the crystallization heat of the undeformed film, to 4−6 J/g for the samples stretched by 200−300%. For the samples with a high tensile strain, in which almost all polymer materials have passed into the fibrillized material of crazes, the crystallization peak disappears on the DSC curve but the high-intensity melting peak remains preserved. Moreover, some samples are characterized by the appearance of a wide endothermic peak (Figure 7b, the curve for tensile strain of 230%) in the temperature range from nearly T_g to the onset of melting. These samples usually lose about 1−3 wt % during the DSC investigation. This peak may be explained by the evaporation of the liquid medium, which may be "sealed" in polymer pores upon the collapse.[30,61] It should be noted that the ΔH_{melt} value weakly depends on the polymer tensile strain and appears to be 35−45 J/g for all deformed samples under investigation.

In spite of the similar deformation behaviors of the PLA film in ethanol and *n*-heptane and the fibrillar−porous structures developed by the crazing mechanism, the patterns of the DSC curves are slightly different. For example, the PLA samples deformed in ethanol are characterized by a shift of the glass-transition temperature toward lower temperature and almost complete disappearance of the endothermic peak (Figure 7a) relevant to the physical aging of the polymer. After PLA is stretched in *n*-heptane, the glass-transition temperature and the area of the endothermic peak in this temperature range are almost equal to those of the initial undeformed film (Figure 7b). It is only for the sample with the tensile strain of 230%, at which the collapse of the crazed structure begin to prevail, that changes in the thermophysical characteristics are observed in the region of T_g. The possible reasons for the observed differences will be discussed below.

Figure 8b shows the dependences of the initial degree of crystallinity of PLA calculated from the difference between the heat effects of melting and crystallization according to formula 2 on the polymer tensile strain upon its deformation in ethanol and *n*-heptane.

It is clearly seen that the degree of crystallinity almost linearly increases with the PLA tensile strain to reach a maximum value of 42−45% at ε = 200−250% irrespective of the nature of the

DOI: 10.1021/acsami.7b09666
ACS Appl. Mater. Interfaces 2017, 9, 34325−34336

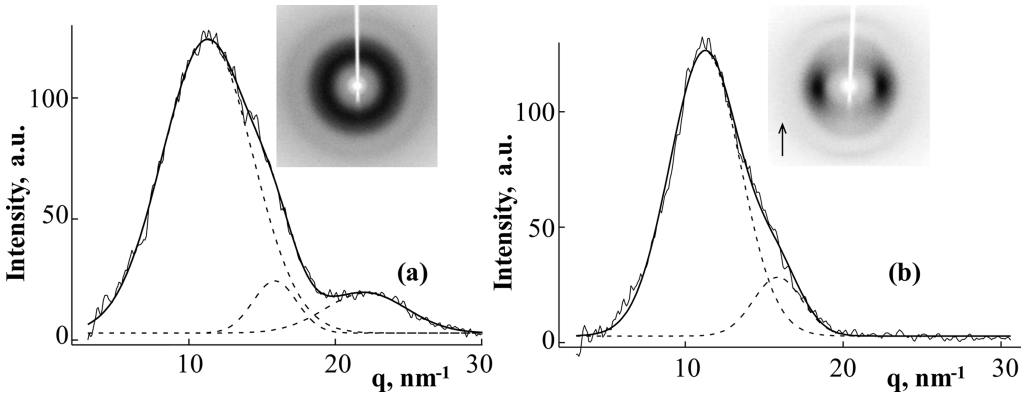

Figure 9. 2D-WAXS patterns, the equatorial radial distributions of scattered X-ray intensity and curve-fitting analysis for (a) the original PLA film and (b) after its uniaxial stretching in air by 250% (region of the neck). The stretching direction is indicated by the arrow.

adsorption-active liquid medium. In Figure 8b, the fraction of the polymer material that has passed into the crazes (f) upon deformation is also presented. This fraction f value is true only if crazing is the main mechanism of sample deformation during drawing. After crazes nucleate and grow through the cross section of a sample, their number remains unchanged. Furthermore, they only widen because of the gradual transfer of a polymer material from the bulk regions into the crazes. As the tensile strain of the polymer material in fibrils is close to its value in the neck, f is given by (see Supporting Information, section S3, page S-6)

$$f = \frac{\varepsilon/100}{\lambda_f - 1} \quad (6)$$

where ε is the tensile strain and λ_f is the draw ratio in fibrils of PLA that equals the draw ratio in the neck (about 3.5).

The curves in Figure 8b obviously show that the degree of crystallinity and the fraction of the polymer material that has passed into the crazes upon deformation grow in a same way. Hence, PLA crystallization during the uniaxial stretching occurs only in the fibrils and does not involve the regions of the bulk polymer.

Thus, the formation of the fibrillary−porous structure in PLA through crazing in liquid media at room temperature is accompanied by spontaneous crystallization of fibrils. Further, we shall consider the influence of a liquid medium and its nature, as well as the polymer orientation, on the low-temperature crystallization of PLA.

To determine the role of a liquid medium in the crystallization of PLA, the maximum degrees of its swelling were measured in ethanol, water−ethanol mixtures, and *n*-heptane. (The experimental swelling curves are presented in the Supporting Information, Figure S3.) The PLA film swelled in ethanol to the maximum degree of about 9% over nearly 24 h under room conditions. Furthermore, the degree of swelling remained unchanged for a month. In 50% water−ethanol mixture, the swelling rate and the maximum degree of swelling of PLA film were significantly lower. In this case, the swelling process continued virtually a month, and the maximum value of 4% was reached after 600 h of soaking. The exposure of PLA in *n*-heptane at room temperature for even a month did not markedly change its mass. To accelerate the swelling process and the attainment of the equilibrium plasticizer concentration, the film was heated in ethanol at a temperature of 50 °C, which is lower than the T_g value and should not induce the crystallization of amorphous PLA. Under these conditions, the swelling rate was substantially increased, and the polymer reached a maximum value of degree of swelling of about 10% in ethanol and about 4% in 50% water−ethanol mixture through 1 h. The equilibrium amount of sorbed ethanol appeared to be almost the same at room temperature and 50 °C. However, the exposure of PLA films in *n*-heptane even at the elevated temperature did not result in its noticeable sorption, thereby indicating that this polymer does not swell in the media of saturated hydrocarbons.

Swelling of a polymer in liquid media is known to decrease its glass-transition temperature that can cause crystallization of an amorphous PLA film even at room temperature. In this work, the glass-transition temperature of PLA was studied as a function of ethanol content using the DSC curves of the wet swollen samples. It was found that the T_g value of PLA with the maximum degree of swelling in ethanol was decreased to 30−35 °C.

The polymer samples after exposure in ethanol and *n*-heptane at room temperature for a month were dried under vacuum and then studied by the DSC technique (experimental DSC curves are presented in Supporting Information, Figure S4a). These data confirm that the thermal transitions and other thermophysical characteristics of the initial PLA film and the one exposed in *n*-heptane actually coincide with each other. However, when heated in the DSC cell, the ethanol-swollen film behaves differently. It intensely starts to crystallize at a temperature 20−30 °C lower than that in the initial sample. One of the possible explanations is that the crystalline phase nuclei form in the sample during its exposure in ethanol. Upon heating, these nuclei play the role of nucleating agents. Moreover, after the polymer was exposed in ethanol for a month, the degree of its crystallinity increased slightly and reached only 8%, thereby indicating a relatively low cold crystallization rate of swollen PLA at room temperature. Thus, the ability of a liquid medium to cause swelling and diffuse into the polymer bulk is not the main factor explaining the glassy PLA crystallization under room conditions.

Earlier, it was reported that uniaxial deformation of PLA samples in air at temperatures lower than T_g (e.g., at 45 °C) did not result in essential crystallization of the polymer.[29] Only stretching above T_g (e.g., at 70−90 °C) yielded samples with a degree of crystallinity as high as 30%. In the present work, we also have obtained samples that uniaxially stretched via necking in air at room temperature to a tensile strain of 250%. The degree of crystallinity of a neck was calculated from DSC data (experimental DSC curves are presented in Supporting

DOI: 10.1021/acsami.7b09666
ACS Appl. Mater. Interfaces 2017, 9, 34325−34336

Information, Figure S4b) as the difference between the heat effects of melting (30 J/g) and crystallization (22 J/g) and was calculated to be nearly 8%, which is slightly higher than that obtained for the bulk PLA film.

Thus, the processes of orientation of a PLA film in air below the glass-transition temperature or its volume swelling in liquid media in the ordinary state do not lead to a notable increase in the crystallinity of the polymer. However, the combined action of a liquid AAM and orienting stress causes rapid crystallization of polymer fibrils at room temperature and results in a material with a high degree of crystallinity (40−45%). Apparently, the penetration of all used environments into the polymer occurred via the formed crazes and did not involve the bulk polymer regions. The bulk polymer swelling over the time of the deformation process (10−20 min) was insignificant (below 1% for unstrained film) even in the presence of ethanol in which the polymer was partially swellable.

3.3. Study of PLA Film Structure Evolution during Low-Temperature Crystallization in Liquid Media. The WAXS method allowed studying the changes in the structure occurring in PLA films during their uniaxial stretching in different media at room temperature and the type of a formed crystalline structure. Figure 9a depicts the 2D scattering pattern and the equatorial radial distribution of scattered X-ray intensity for an initial PLA film. The X-ray pattern exhibits a diffuse (amorphous) halo with uniform intensity distribution over the circle. The scattering curve shows a rather intense and wide halo in a scattering vector range of 3−19 nm^{-1} and a less intense halo with a maximum at $q \approx 23$ nm^{-1}. The fitting procedure reveals three halos located at q = 11.3, 15.9, and 22.1 nm^{-1}, with nearly equal values of fwhm ≈ 5−7 nm^{-1}. Previously, the unification of two amorphous halos into one wide scattering peak[5] was, by analogy with PET, explained by the presence of two characteristic interchain spacings in amorphous PLA.

When considering the thermophysical properties, we have already noted that the PLA orientation by uniaxial stretching leads to increase of crystallinity degree in the neck only to 8%. The WAXS pattern obtained for a region of the neck (Figure 9b) exhibits two symmetric diffuse spots at the equator, with no crystalline reflections observed. This finding confirms that, as a result of the cold stretching, the PLA film acquires an oriented structure but remains virtually amorphous. The curve for scattering in the equatorial direction (Figure 8b) also shows a rather intense and very wide peak in a range of scattering vector values of 3−19 nm^{-1} but the peripheral peak in the region of the third-layer line is negligible. The fitting procedure has confirmed that the positions of the amorphous halo maxima remain unchanged, while the values of the Gaussian fwhms markedly decrease to approximately 4−5.5 nm^{-1}. This fact may indicate the formation of ordered domains during drawing, which can be regarded as the nuclei of a crystalline phase or the so-called mesophase (mesocrystal).[23,29]

Both the DSC studies and WAXS data (Figure 10) have shown that the uniaxial deformation of PLA films in both ethanol and *n*-heptane, in which PLA is swellable and nonswellable, respectively, is accompanied by low-temperature crystallization. Figure 11 depicts the 2D-WAXS pattern and the corresponding scan with the assignment of all reflections for the sample deformed in a liquid medium. At tensile strains below 50%, when the fraction of the film area occupied by crazes is small, distinct arc-shaped reflections corresponding to (200)/(110) and (203) planes arise at the equator and at an angle of

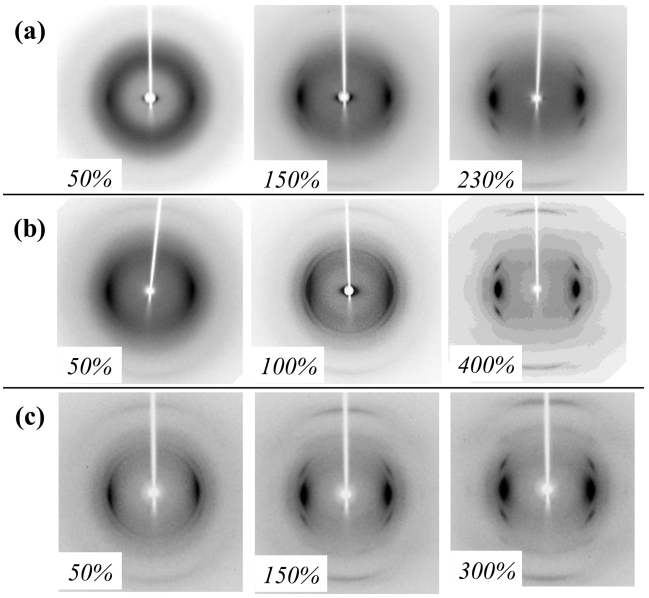

Figure 10. 2D-WAXS patterns of the PLA film after uniaxial strain in the presence of (a) *n*-heptane, (b) 50% water−ethanol mixture, and (c) ethanol at room temperature. The tensile strains of samples are shown on patterns. Stretching direction is vertical for all samples.

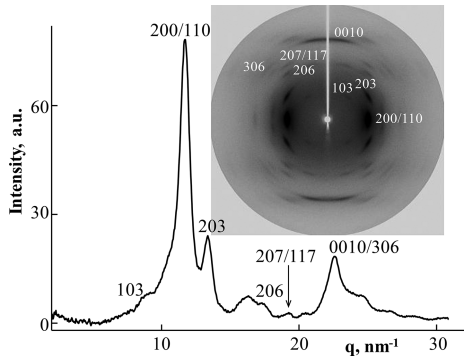

Figure 11. 2D-WAXS pattern and the corresponding azimuth-integrated distribution curve of the scattered intensity for the PLA film stretched by 400% in 50% water−ethanol mixture at room temperature.

nearly 30°. They indicate the presence of the crystalline phase with α and α'-orthorhombic lattices. According to the published data,[62] the α phase must, in addition to (200)/(110) and (203) reflections, have pronounced equatorial (010) and (210) reflections. When these reflections are absent or weakly pronounced, the α' phase is commonly believed to be formed. As the tensile strain grows, the intensity of the amorphous halo decreases, while the reflections from crystallites become more distinct and diagonal (203) reflections become noticeable. This occurs because of both a rise in the fraction of the polymer that has passed into the crazes and the improvement of crystallinity. The PLA samples were stretched to a high tensile strain (more than 200%), in which most of the area of the polymer material has passed to the fibrillar state and the structural rearrangements relevant to the collapse of the porous structure have begun. They show an axial texture with high degrees of crystallinity and molecular orientation. To confirm the formation of a highly ordered structure of PLA during crazing, the disorientation angle of PLA crystallites with respect to the direction of elongation was defined by WAXS

DOI: 10.1021/acsami.7b09666
ACS Appl. Mater. Interfaces 2017, 9, 34325−34336

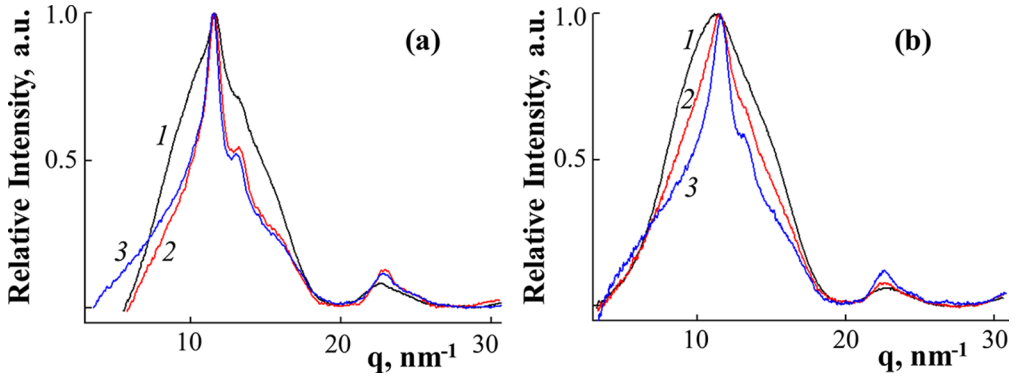

Figure 12. The azimuth-integrated distribution curves of the scattered intensity for the PLA film after uniaxial stretching in the presence of (a) ethanol (the tensile strains of 50 (1), 150 (2), and 300% (3)) and (b) *n*-heptane (the tensile strains of 50 (1), 150 (2), and 230% (3)) at room temperature.

data. This parameter characterizes the degree of ordering of the crystalline phase in a selected direction. It has been determined that the value of a disorientation angle for PLA samples with a tensile strain of 250−400% is 12°−17° irrespective of the type of the liquid environment. Thus, a sufficiently high degree of orientation of the crystalline phase develops during crazing.

It should be noted that the 2D-WAXS patterns for samples that have been crystallized upon deformation in media, which are unable (*n*-heptane) and able (ethanol) to cause polymer swelling, are slightly different (Figure 10a,c, respectively). This may be related to different rates of PLA crystallization, because the glass-transition temperature of the polymer swollen in ethanol is substantially (up to 30−35 °C) decreased because of the plasticizing action of ethanol. Moreover, under the same conditions of stretching, the concentration of the crazes formed per unit length of the working part in ethanol is much smaller than that in *n*-heptane or an aqueous 50% ethanol solution because of the lower plastic yielding value. Therefore, at formally equal tensile strains of macromolecules, the real tensile strain in crazes developed in ethanol is higher at lower ε values. However, because at high tensile strains (above 200%) the degree of PLA crystallinity is equal to both media, thermodynamic criteria for the possibility of crystallization are implemented.

In Figure 12, the scans obtained from 2D-WAXS patterns are presented. The samples deformed to a tensile strain of 50% (curves 1) are characterized by very wide peaks similar to that presented in Figure 9a for the initial isotropic film. As the tensile strain of PLA in ethanol and *n*-heptane grows, reflections from (200)/(110), (203), and (0010/306) planes at the corresponding values q = 11.7, 13.2, and 22.8 nm^{-1} arise and become more evident in the scattering curves, while the fwhm values of the peaks decrease to 1−2 nm^{-1} at unchanged angular positions of the maxima.

The degrees of crystallinity calculated from the fitted WAXS data have appeared to differ substantially from the values determined by DSC. The possible reason is structural nonuniformity (irregular alternation of undeformed bulk regions and crazes). The fractions of the bulk and crazed parts that occur in the studied region, as well as the fraction of the crazed material, cannot be accurately controlled because the size of the X-ray beam is as small as 300 × 300 μm. This was confirmed by WAXS patterns obtained from the different parts of the same sample stretched by 50% in ethanol (the data are presented in Supporting Information, Figure S5). While one pattern was identical to the initial amorphous sample, the other one clearly exhibited crystalline reflections. For similar structurally nonuniform crazed systems, good coincidence was observed only in the case of samples deformed to high tensile strains (300−400%), at which almost all polymer materials had passed into the crazes. For example, in the case of a PLA sample deformed by 300% in ethanol, the degrees of crystallinity determined from the DSC and WAXS data were 43 and 45%, respectively.

The calculation of crystallite sizes from the (200)/(110) plane has shown that they depend on the nature of the aqueous medium in which crazing is performed. However, they remain almost unchanged upon increasing the tensile strain. In ethanol, which causes partial swelling, the crystallite size appeared to be 5−5.5 nm, while, in *n*-heptane, which causes no swelling, it was slightly smaller, that is, 3−3.5 nm.

Thus, deformation of an isotropic glassy PLA film in liquid AAMs is accompanied by an intense crystallization of the fibrillar material filling crazes yielding α'-crystalline phase characterized by a rather high degree of orientation in the direction of elongation.

On the basis of the obtained experimental data, crystallization of glassy polylactide under room conditions during drawing in liquid AAMs can be represented in the following way. The application of a uniaxial tensile stress to the PLA film in the presence of a liquid environment initiates the development of deformation by the crazing mechanism. The liquid considerably reduces the surface energy of a polymer by wetting, which significantly (several times) reduces the mechanical stress at which drawing occurs and stabilizes obtained fibrils with nanoscale diameter of 10−20 nm generated in crazes. These polymeric nanoscale objects, namely, fibers, films, and surface layers with thickness less than 30−40 nm, may possess significantly reduced glass-transition temperature. For example, it was previously shown[62−65] that thin films of various glassy polymers (polystyrene and poly(methylmethacrylate)) are characterized by decreased T_g value by a few tens of degrees. Furthermore, it was suggested[40,54] that mobility of polymer chains at the craze−bulk polymer boundary was strongly enhanced by the presence of the triaxial tensile stress at the base of each craze fibril. Therefore, the T_g of PLA in fibrils could be reduced to room temperature. The combination of a sufficient level of mobility of the macromolecules and their orientation in the fibrils, promotes spontaneous cold crystallization of a glassy polymer. While tensile strain increases and the fraction of the polymeric material passes into the crazes, the polymer crystallinity

DOI: 10.1021/acsami.7b09666
ACS Appl. Mater. Interfaces 2017, 9, 34325−34336

increases. This process proceeds continuously until the bulk parts of the PLA film are transferred into crazes. The engineer tensile strain reaches the natural tensile strain of the polymer, in this case up to 250% with a formation of the structure of highly oriented and crystalline fibrils. Therefore, the "cold" crystallization involves only fibrils bearing craze walls and does not occur in the regions of the bulk polymer. Further elongation process (above 250%) does not change the degree of crystallinity of the polymer and results only in the improvement of a preliminary-formed crystalline structure until the strain at break.

The reinforcement of PLA fibrils with the formed crystalline phase seems to stabilize the development of the crazed structure in the polymer up to high tensile strains. Moreover, the deformability of PLA, which is rather brittle at room temperature, increases in some cases to values higher than 500%. This possible stabilizing action of the crystallization of a polymer or a crystallizable component of a blend to fibrils formed in crazes was mentioned by Kambour.[66]

4. CONCLUSIONS

In this work, it has been discovered for the first time that the development of a finely dispersed structure of the fibrillar material in PLA films upon crazing in liquid AAMs (ethanol, water−ethanol mixtures, and *n*-heptane) leads to intense crystallization of the glassy polymer under room conditions (below its glass-transition temperature). We have shown correlation between the amount of a fibrillar material and the degree of crystallinity. The degree of crystallinity increases with an increase in the fraction of PLA that has passed into the region of the fibrillar material. Under chosen conditions, the maximum degree of crystallinity reaches 45%. Therewith, the crystallization process is accompanied by the formation of an α'-crystalline phase, which is more disordered than the relevant α-phase. The size of the formed PLA crystallites depends on the nature of an AAM and amounts to about 3−5 nm. Therefore, the crystallization of PLA nanofibrils in the crazes leads to their stabilization and imparts high deformability to the polymer. Such an orientational stretching in the presence of liquid media allowed increasing the tensile strength of the PLA film by 3 times.

The described effect of cold crystallization under the combined action of a liquid medium and orienting stress has been previously revealed for amorphous films and fibers of PET and for mixed films of phthalate polyester and bisphenol A polycarbonate. Thus, it can be stated as the discovery of some phenomenon having a fundamental character as applied to amorphous polymers that are capable of crystallization. This process may be of great interest for applied fields because it offers opportunities for the preparation of the polymer materials and their composites with variable structural and mechanical properties.

■ ASSOCIATED CONTENT

Supporting Information

The Supporting Information is available free of charge on the ACS Publications website at DOI: 10.1021/acsami.7b09666.

The 2D SAXS patterns of the initial PLA film and the sample stretched by 50% in ethanol; description of the mathematical methods of calculation of the PLA fibril diameter and the fraction of a polymer material that has passed into the crazes; experimental swelling curves; and experimental DSC curves of the different PLA samples (PDF)

■ AUTHOR INFORMATION

Corresponding Authors

*E-mail: elena_trofimchuk@mail.ru (E.S.T.).
*E-mail: s-chvalun@yandex.ru (S.N.C.).

ORCID

Elena S. Trofimchuk: 0000-0002-8035-7872
Ekaterina G. Rukhlya: 0000-0001-5506-654X

Notes

The authors declare no competing financial interest.

■ ACKNOWLEDGMENTS

This work has been financially supported by the Russian Foundation for Basic Research (project 16-03-00504) and by President's grant for young scientists (project MK-2878.2017.3). X-ray measurements has been performed at the unique scientific facility of the Kurchatov Synchrotron Radiation Source supported by the Ministry of Education and Science of the Russian Federation (project RFME-FI61917X0007).

■ REFERENCES

(1) Inkinen, S.; Hakkarainen, M.; Albertsson, A.-C.; Södergård, A. From Lactic Acid to Poly(lactic acid) (PLA): Characterization and Analysis of PLA and Its Precursors. *Biomacromolecules* **2011**, *12*, 523−532.

(2) Ren, J. *Biodegradable Poly(Lactic Acid): Synthesis, Modification, Processing, and Applications*; Springer: Berlin, 2010; p 302.

(3) Hamad, K.; Kaseem, M.; Yang, H. W.; Deri, F.; Ko, Y. G. Properties and Medical Applications of Polylactic Acid: A Review. *eXPRESS Polym. Lett.* **2015**, *9*, 435−455.

(4) Goh, K.; Heising, J. K.; Yuan, Y.; Karahan, H. E.; Wei, L.; Zhai, S.; Koh, J.-X.; Htin, N. M.; Zhang, F.; Wang, R.; Fane, A. G.; Dekker, M.; Dehghani, F.; Chen, Y. Sandwich-Architectured Poly(lactic acid)−Graphene Composite Food Packaging Films. *ACS Appl. Mater. Interfaces* **2016**, *8*, 9994−10004.

(5) *Poly(Lactic Acid): Synthesis, Structures, Properties, Processing, and Applications*; Auras, R., Lim, L.-T., Selke, S. E. M., Tsuji, H., Eds.; Wiley: New York, Hoboken, 2010; p 499.

(6) Garlotta, D. A Literature Review of Poly(lactic acid). *J. Polym. Environ.* **2001**, *9*, 63−84.

(7) Celli, A.; Scandola, M. Thermal properties and physical ageing of poly(L-lactic acid). *Polymer* **1992**, *33*, 2699−2703.

(8) Lim, L.-T.; Auras, R.; Rubino, M. Processing technologies for poly(lactic acid). *Prog. Polym. Sci.* **2008**, *33*, 820−852.

(9) Kulinski, Z.; Piorkowska, E.; Gadzinowska, K.; Stasiak, M. Plasticization of Poly(L-lactide) with Poly(propylene glycol). *Biomacromolecules* **2006**, *7*, 2128−2135.

(10) Rasal, R. M.; Janorkar, A. V.; Hirt, D. E. Poly(lactic acid) Modifications. *Prog. Polym. Sci.* **2010**, *35*, 338−356.

(11) Xie, L.; Xu, H.; Niu, B.; Ji, X.; Chen, J.; Li, Z.-M.; Hsiao, B. S.; Zhong, G.-J. Unprecedented Access to Strong and Ductile Poly(lactic acid) by Introducing In Situ Nanofibrillar Poly(butylene succinate) for Green Packaging. *Biomacromolecules* **2014**, *15*, 4054−4064.

(12) Gámez-Pérez, J.; Velazquez-Infante, J. C.; Franco-Urquiza, E.; Pages, P.; Carrasco, F.; Santana, O. O.; Maspoch, M. L. Fracture Behavior of Quenched Poly(lactic acid). *eXPRESS Polym. Lett.* **2011**, *5*, 82−91.

(13) Huang, T.; Miura, M.; Nobukawa, S.; Yamaguchi, M. Chain Packing and Its Anomalous Effect on Mechanical Toughness for Poly(lactic acid). *Biomacromolecules* **2015**, *16*, 1660−1666.

(14) Kfoury, G.; Raquez, J.-M.; Hassouna, F.; Odent, J.; Toniazzo, V.; Ruch, D.; Dubois, P. Recent Advances in High Performance

Poly(lactide): From "Green" Plasticization to Super-Tough Materials via (Reactive) Compounding. *Front. Chem.* **2013**, *1*, 32.
(15) Yu, L.; Liu, H.; Xie, F.; Chen, L.; Li, X. Effect of Annealing and Orientation on Microstructures and Mechanical Properties of Polylactic acid. *Polym. Eng. Sci.* **2008**, *48*, 634−641.
(16) Geng, L.; Li, L.; Mi, H.; Chen, B.; Sharma, P.; Ma, H.; Hsiao, B. S.; Peng, X.; Kuang, T. Superior Impact Toughness and Excellent Storage Modulus of Poly(lactic acid) Foams Reinforced by Shish-Kebab Nanoporous Structure. *ACS Appl. Mater. Interfaces* **2017**, *9*, 21071−21076.
(17) Hoogsteen, W.; Postema, A. R.; Pennings, A. J.; Ten Brinke, G.; Zugenmaier, P. Crystal Structure, Conformation, and Morphology of Solution-Spun Poly(L-lactide) Fibers. *Macromolecules* **1990**, *23*, 634−642.
(18) Tsuji, H.; Ikada, Y. Properties and Morphologies of Poly(L-lactide): 1. Annealing Condition Effects on Properties and Morphologies of Poly(L-lactide). *Polymer* **1995**, *36*, 2709−2716.
(19) Bai, H.; Zhang, W.; Deng, H.; Zhang, Q.; Fu, Q. Control of Crystal Morphology in Poly(L-lactide) by Adding Nucleating Agent. *Macromolecules* **2011**, *44*, 1233−1237.
(20) Zhou, S.-Y.; Niu, B.; Xie, X.-L.; Ji, X.; Zhong, G.-J.; Hsiao, B. S.; Li, Z.-M. Interfacial Shish-Kebabs Lengthened by Coupling Effect of In Situ Flexible Nanofibrils and Intense Shear Flow: Achieving Hierarchy To Conquer the Conflicts between Strength and Toughness of Polylactide. *ACS Appl. Mater. Interfaces* **2017**, *9*, 10148−10159.
(21) Guan, Y.; Liu, G.; Ding, G.; Yang, T.; Müller, A. J.; Wang, D. Enhanced Crystallization from the Glassy State of Poly(L-lactic acid) Confined in Anodic Alumina Oxide Nanopores. *Macromolecules* **2015**, *48*, 2526−2533.
(22) De Santis, P.; Kovacs, A. J. Molecular Conformation of Poly(S-lactic acid). *Biopolymers* **1968**, *6*, 299−306.
(23) Zhou, C.; Li, H.; Zhang, W.; Li, J.; Huang, S.; Meng, Y.; de Claville Christiansen, J.; Yu, D.; Wu, Z.; Jiang, S. Direct Investigations on Strain-Induced Cold Crystallization Behavior and Structure Evolutions in Amorphous Poly(lactic acid) with SAXS and WAXS Measurements. *Polymer* **2016**, *90*, 111−121.
(24) Eling, B.; Gogolewski, S.; Pennings, A. J. Biodegradable Materials of Poly(L-lactic acid): 1. Melt-Spun and Solution-Spun Fibres. *Polymer* **1982**, *23*, 1587−1593.
(25) Sawai, D.; Takahashi, K.; Imamura, T.; Nakamura, K.; Kanamoto, T.; Hyon, S.-H. Preparation of Oriented β-Form Poly(L-lactic acid) by Solid-State Extrusion. *J. Polym. Sci., Part B: Polym. Phys.* **2002**, *40*, 95−104.
(26) Stoclet, G.; Seguela, R.; Lefebvre, J. M.; Elkoun, S.; Vanmansart, C. Strain-Induced Molecular Ordering in Polylactide upon Uniaxial Stretching. *Macromolecules* **2010**, *43*, 1488−1498.
(27) Zhou, C.; Li, H.; Zhang, Y.; Xue, F.; Huang, S.; Wen, H.; Li, J.; de Claville Christiansen, J.; Yu, D.; Wu, Z.; Jiang, S. Deformation and Structure Evolution of Glassy Poly(lactic acid) Below the Glass Transition Temperature. *CrystEngComm* **2015**, *17*, 5651−5663.
(28) Zhang, J.; Duan, Y.; Domb, A. J.; Ozaki, Y. PLLA Mesophase and Its Phase Transition Behavior in the PLLA-PEG-PLLA Copolymer as Revealed by Infrared Spectroscopy. *Macromolecules* **2010**, *43*, 4240−4246.
(29) Stoclet, G.; Seguela, R.; Lefebvre, J.-M.; Rochas, C. New Insights on the Strain-Induced Mesophase of Poly(D,L-lactide): In Situ WAXS and DSC Study of the Thermo-Mechanical Stability. *Macromolecules* **2010**, *43*, 7228−7237.
(30) Volynskii, A. L.; Bakeev, N. F. *Solvent Crazing of Polymers*; Elsevier: Amsterdam, NY, 1995; p 413.
(31) Kawagoe, M.; Ishimi, T. On the Properties of Organic Liquids Affecting the Crazing Behaviour in Glassy Polymers. *J. Mater. Sci.* **2002**, *37*, 5115−5121.
(32) De Focatiis, D. S. A.; Buckley, C. P.; Hutchings, L. R. Roles of Chain Length, Chain Architecture, and Time in the Initiation of Visible Crazes in Polystyrene. *Macromolecules* **2008**, *41*, 4484−4491.
(33) Rottler, J.; Robbins, M. O. Growth, Microstructure, and Failure of Crazes in Glassy Polymers. *Phys. Rev. E: Stat., Nonlinear, Soft Matter Phys.* **2003**, *68*, 011801.
(34) Argon, A. S. Craze initiation in glassy polymers—Revisited. *Polymer* **2011**, *52*, 2319−2327.
(35) Trofimchuk, E. S.; Nikonorova, N. I.; Chagarovskii, A. O.; Volynskii, A. L.; Bakeev, N. F. Crystallization of Silver Chloride in Crazed Porous Polymers. *J. Phys. Chem. B* **2005**, *109*, 16278−16283.
(36) Trofimchuk, E. S.; Nesterova, E. A.; Meshkov, I. B.; Nikonorova, N. I.; Muzafarov, A. M.; Bakeev, N. P. Polypropylene/Silicate Composites on the Basis of Crazed Polymer and Hyperbranched Polyethoxysiloxane. *Macromolecules* **2007**, *40*, 9111−9115.
(37) Goel, P.; Vinokur, R.; Weichold, O. Current-Dependent Anisotropic Conductivity of Locally Assembled Silver Nanoparticles in Hybrid Polymer Films. *J. Colloid Interface Sci.* **2010**, *352*, 343−347.
(38) Yarysheva, L. M.; Rukhlya, E. G.; Yarysheva, A. Y.; Volynskii, A. L.; Bakeev, N. F. Crazing as a Method for Preparation of Polymer Blends. *Rev. J. Chem.* **2012**, *2*, 1−19.
(39) Trofimchuk, E. S.; Mal'tsev, D. K.; Sedush, N. G.; Efimov, A. V.; Nikonorova, N. I.; Grokhovskaya, T. E.; Chvalun, S. N.; Volynskii, A. L.; Bakeev, N. F. Features of Uniaxial Tension of Amorphous Poly-L-Lactic Acid in Liquid Media. *Dokl. Phys.* **2014**, *59*, 568−571.
(40) Yefimov, A. V.; Shcherba, V. Y.; Ozerin, A. N.; Rebrov, A. V.; Bakeyev, N. F. The Structure of Crazing Formed as a Result of Deformation in Polyethyleneterephthalate at Various Temperatures. *Polym. Sci. U.S.S.R.* **1990**, *32*, 769−775.
(41) Sinevich, E. A.; Prazdnichnyi, A. M.; Bakeev, N. F. Application of a New Method for the Determination of Structural Parameters of "Wet" Crazes to Gain Insight into the Mechanism of Solvent Crazing in Polymers. *Polym. Sci., Ser. A* **1996**, *38*, 159−163.
(42) Khanum, R.; Takarada, W.; Aneja, A.; Kikutani, T. Crystallization of Poly(ethylene terephthalate) Filaments by Infusion of Ethanol upon Cold Drawing. *Polymer* **2015**, *59*, 26−34.
(43) Fadeeva, I. V.; Trofimchuk, E. S.; Giretova, M.; Mal'tsev, D. K.; Nikonorova, N. I.; Fomin, A. S.; Rau, J. V.; Medvecky, L.; Barinov, S. M. Novel Approach to Obtain Composite Poly-L-Lactide Based Films Blended with Starch and Calcium Phosphates and their Bioactive Properties. *Biomed. Phys. Eng. Express* **2015**, *1*, 045011.
(44) Fischer, E. W.; Sterzel, H. J.; Wegner, G. Investigation of the Structure of Solution Grown Crystals of Lactide Copolymers by Means of Chemical Reactions. *Kolloid Z. Z. Polym.* **1973**, *251*, 980−990.
(45) Klug, H. P.; Alexander, L. E. *X-ray Diffraction Procedures: For Polycrystalline and Amorphous Materials*, 2nd ed.; John Wiley & Sons: New York, 1974; p 992.
(46) Korneev, V. N.; Sergienko, P. M.; Matyushin, A. M.; Shlektarev, V. A.; Ariskin, N. I.; Shishkov, V. I.; Gorin, V. P.; Sheromov, M. A.; Aul'chenko, V. M.; Zabelin, A. V.; Stankevich, V. G.; Yudin, L. I.; Vazina, A. A. Current Status of the Small-Angle Station at Kurchatov Center of Synchrotron Radiation. *Nucl. Instrum. Methods Phys. Res., Sect. A* **2005**, *543*, 368−374.
(47) Huang, T. C.; Toraya, H.; Blanton, T. N.; Wu, Y. X-Ray Powder Diffraction Analysis of Silver Behenate, a Possible Low-Angle Diffraction Standard. *J. Appl. Crystallogr.* **1993**, *26*, 180−184.
(48) Renouf-Glauser, A. C.; Rose, J.; Farrar, D. F.; Cameron, R. E. Comparison of the Hydrolytic Degradation and Deformation Properties of a PLLA−Lauric Acid Based Family of Biomaterials. *Biomacromolecules* **2006**, *7*, 612−617.
(49) Narisawa, I.; Yee, A. In *Crazing and Fracture of Polymers, Structure and Properties of Polymers, Materials Science and Technology, a Comprehensive Treatment*; Thomas, E. L., Ed.; VCH: Weinheim, 1993; Vol. *12*, pp 698−765.
(50) Gearing, B. P.; Anand, L. On Modeling the Deformation and Fracture Response of Glassy Polymers Due to Shear-Yielding and Crazing. *Int. J. Solid Struct.* **2004**, *41*, 3125−3150.
(51) *Encyclopedia of Polymer Science and Technology*, 3rd ed.; Mark, H. F., Ed.; John Wiley & Sons, Inc.: Hoboken, NY, 2003; Vol. *1*, pp 290−317.
(52) *The Physics of Glassy Polymers*; Haward, R. N., Young, R. J., Eds.; Chapman & Hall: Springer Netherlands, 1997; p 508.

DOI: 10.1021/acsami.7b09666
ACS Appl. Mater. Interfaces 2017, 9, 34325−34336

(53) Senden, D. J. A.; Engels, T. A. P.; Söntjens, S. H. M.; Govaert, L. E. The Effect of Physical Aging on the Embrittlement of Steam-Sterilized Polycarbonate. *J. Mater. Sci.* **2012**, *47*, 6043−6046.
(54) Kramer, E. J. Microscopic and Molecular Fundamentals of Crazing. In *Crazing in Polymers*; Kausch, H. H., Ed.; Advances in Polymer Science; Springer: Berlin, 1983; Vol. *52/53*, pp 1−56.
(55) Yarysheva, L. M.; Dolgova, A. A.; Arzhakova, O. V.; Volynskii, A. L.; Bakeev, N. F. The Effect of the Nature of a Liquid Medium on the Rates of Craze Tip Advance and Craze Widening in Poly(ethylene terephthalate). *Polym. Sci., Ser. A* **2002**, *44*, 865−871.
(56) Volynskii, A. L.; Loginov, V. S.; Bakeyev, N. F. Structure and Adsorption Properties of the Material of Crazes in Glassy Polyethylene Terephthalate. *Polym. Sci. U.S.S.R.* **1981**, *23*, 1350−1356.
(57) Yarysheva, L.; Volynskii, A.; Bakeev, N. Environmental Crazing as a Method of Preparation of Porous Materials. *Vysokomolekulyarnye Soedineniya Ser. B* **1993**, *35*, 913−921.
(58) Arzhakova, O. V.; Dolgova, A. A.; Yarysheva, L. M.; Volynskii, A. L.; Bakeev, N. F. Specific Features of the Environmental Crazing of Poly(ethylene Terephthalate) Fibers. *Polymer* **2015**, *56*, 256−262.
(59) Volynskii, A. L.; Bakeev, N. F. *Surface Phenomena in the Structural and Mechanical Behaviour of Solid Polymers*; CRC Press, Taylor & Francis Group, 2016; p 536.
(60) Paredes, E.; Fischer, E. W. Röntgenkleinwinkel-untersuchungen zur struktur der crazes (fließzonen) in polycarbonat und poly-methylmethacrylate. *Makromol. Chem.* **1979**, *180*, 2707−2722.
(61) Yarysheva, A. Y.; Rukhlya, E. G.; Yarysheva, L. M.; Bagrov, D. V.; Volynskii, A. L.; Bakeev, N. F. The Structural Evolution of High-Density Polyethylene During Crazing in Liquid Medium. *Eur. Polym. J.* **2015**, *66*, 458−469.
(62) Zhang, J.; Tashiro, K.; Tsuji, H.; Domb, A. J. Disorder-to-Order Phase Transition and Multiple Melting Behavior of Poly(L-lactide) Investigated by Simultaneous Measurements of WAXD and DSC. *Macromolecules* **2008**, *41*, 1352−1357.
(63) Forrest, J. A.; Dalnoki-Veress, K. The Glass Transition in Thin Polymer Films. *Adv. Colloid Interface Sci.* **2001**, *94*, 167−195.
(64) Kim, J. H.; Jang, J.; Zin, W.-C. Thickness Dependence of the Glass Transition Temperature in Thin Polymer Films. *Langmuir* **2001**, *17*, 2703−2710.
(65) Zhang, C.; Guo, Y.; Priestley, R. D. Confined Glassy Properties of Polymer Nanoparticles. *J. Polym. Sci., Part B: Polym. Phys.* **2013**, *51*, 574−586.
(66) Kambour, R. P.; Chu, C.; Avakian, R. W. Crystallizing Crazes: The Probable Source of Solvent Stress Cracking Resistance in a Polyester/Polycarbonate Blend. *J. Polym. Sci., Part B: Polym. Phys.* **1986**, *24*, 2135−2144.

DOI: 10.1021/acsami.7b09666
ACS Appl. Mater. Interfaces 2017, 9, 34325−34336